Journal of Materials and Engineering Structures

Research Paper

The Performance of Monolithic Reinforced Concrete Structure Includes Slab, Beam and Column against Blast Load

K. Senthil*, S. Rupali, Navjit Kaur

Department of Civil Engineering, National Institute of Technology Jalandhar, Punjab 144011, India

ARTICLE INFO

Article history :

Received : 27 January 2018

Revised : 20 May 2018

Accepted : 21 May 2018

Keywords:

Blast Load

Finite Element Analysis

Standoff Distance

Deformation and Stresses

ABSTRACT

The numerical investigations has been carried out on reinforced concrete structures against blast loading to demonstrate the accuracy and effectiveness of the finite element based numerical models. The size of building was considered 3 ×3 × 3 m and whereas the size of beam and column was 0.3 m, arbitrary. The thickness of roof slab was 120 mm, whereas the reinforced concrete wall on all four sides was 0.2 m. The simulations were carried out through finite element code ABAQUS/CAE. The inelastic behavior of concrete has been incorporated through concrete damage plasticity model and the model includes compressive and tensile behavior. The elastic and plastic behavior of steel reinforcement bar has been incorporated using Johnson-cook model includes the effect of state of stress, temperature and strain rate. The simulations were carried out against varying standoff distance, mass of TNT, locations of blast origin and thickness of roof slab to examine the resistance of building. The response of structural elements were studied in light of deflection, impulsive velocity, von-Mises stresses, compression and tension damage of concrete. The results indicate that the standoff distance has great influence on the survivability of reinforced concrete slab and wall.

1 Introduction

Due to increasing terrorist attacks over the past decades the effect of blast loads on the structure is a serious matter of concern that should be taken into consideration in the design process. Various studies were conducted in the past to predict the behaviour of structural reinforced concrete elements under blast loading. Nowadays, a numerical model for the blast load assessment are starting to become more accurate and reliable. This is because the computational time for such an assessment has been reduced to satisfactory level. Elsanadedy et al. [1] carried out an experiment to study the effect of blast load generated on the existing exterior RC circular columns. The effect of stand-off distance, charge weight and the pressure CFRP retrofitting were studied through parametric studies using non-linear finite element analysis software LS-DYNA. It was observed that CFRP strengthening could be an effective solution to eliminate the damage caused by moderate explosions. Crawford et al. [2] conducted finite element analyses of 1.10 m diameter circular reinforced concrete column was retrofitted

* *Corresponding author. Tel.: +91-9458948743.*
E-mail address: urssenthil85@yahoo.co.in; kasilingams@nitj.ac.in

e-ISSN: 2170-127X, (cc) BY-SA

RESEARCH REVIEW of Sciences and Technologies

with CFRP composites against 682 and 1364 kg TNT charges at 3.05, 6.1 and 12.2 m stand-off distances. An explosive loading was applied and a pressure at the top of the column was used to simulate the upper stories. All results showed that composite retrofits could have a beneficial effect on the performance of the columns and therefore prevent progressive collapse. The retrofitting was shown to reduce the lateral displacement considerably. Ahmad et al. [3] carried out experiments on four different RC walls with varying thickness for different explosive loads and scaled distance. It was concluded that air blast and ground shock pressure are important for accurate analysis of structural response of structure.

Woodson et al. [4] tested a number of reinforced concrete slabs to ascertain the stirrups requirement for blast resistance. The slabs were loaded to a very large uniform pressure in a gas chamber and the responses in term of support rotation were measured. The results of these tests indicated that the requirement for shear reinforcements in the blast resistant manual are highly conservative and suggested an effective way of improving the ductility at a lesser cost. The experiments though could produce pressures equivalent to a blast, the pressure-time history could not be simulated for a realistic situation. Shi et al. [5] also conducted numerical investigations to investigate the bond-slip effect on numerical analysis of blast-induced responses of a RC column. Samir [6] performed numerical simulations on reinforced concrete columns subjected to various blast loads using the finite element software ABAQUS. The effects of transverse and longitudinal reinforcement ratios, charge weight and column aspect ratio were the parameters considered. It was concluded that the residual displacement becomes more significant after a certain charge weight. King et al. [7] discussed typical building retrofit strategies for load bearing and nonload bearing structural members through strengthening, shielding, or controlling hazardous debris.

Ngo [8] presents a comprehensive overview of the effects of explosion on structures. An explanation of the nature of explosions and the mechanism of blast waves in free air is given. Authors were introduced different methods to estimate blast loads and structural response. Watson et al. [9] carried out experiments and measured the damages caused to reinforced concrete T beams and slabs by contact and close proximity explosive charges using different areas of contact and angles of inclination for the explosives. Experiments of blast on the prototype and model specimens were conducted and found in agreement between the prototype and model response. Wakchaure and Borole [10] discuss the comparison between long side and short side column is made and percentage of stress of reinforced concrete column for long and short side is presented an analysis is done in ANSYS. It was conclude that the critical impulse for the long column case found to be significantly higher.

Ellis and Crowhurst [11] carried out an experimental study for the elastic response of panels to gas explosions. A large scale explosion test facility was developed to conduct the tests with sophisticated instrumentation. A single degree of freedom system elastic model was adopted to predict the response of the panel analytically. The results compared well indicating that if the dynamic characteristics of any panel can be measured accurately, then the response of the panel to a given explosion can be determined accurately. Sagaseta et al. [12] studied the effect of Punching shear failure in RC slabs and panels subjected to blast loads. It is observed that the distribution of reflected overpressure on the RC slabs is exponentially decaying. It is also observed that the close-range blasts can result in punching shear failures adjacent to the detonation in RC slabs or panels due to the localised loading and high shear demand in this region during the short load duration. This paper proposes a methodology by which punching shear failures can be assessed and the approach has been validated using tests with scale distances between 0.2 and 1.5 m/kg$^{1/3}$.

Based on the detailed literature survey, it is observed that most studies focused on elements of structures such as slab, column and T beam subjected to blast loading. The lack of understanding is mainly due to the complexity of the problem where too many variables involves and the response of elements alone do not lead to effective design methods. Also it is observed that the behaviour of concrete using concrete damage plasticity model against blast loading is limited. The performance of monolithic reinforced structure includes slab, beam and column against blast loading is found limited heretofore. Hence, present numerical study is focused on simulations of various structural elements composed in together against blast loading to address the behaviour of monolithic structure. In the present study, the numerical investigations has been carried out on reinforced concrete structures against blast loading through finite element code ABAQUS/CAE. The size of building was considered 3 x 3 x 3 m and whereas the cross section of beam and column was 0.3 m, arbitrary. The thickness of roof slab was 120 mm, whereas the reinforced concrete wall all four sides was 0.2 m. The inelastic behavior of concrete and steel reinforced bar has been incorporated through concrete damage plasticity model and Johnson-cook model respectively. The simulations were carried out against varying standoff distance, mass of TNT, locations of blast origin and thickness of roof slab. The response of structural elements were studied in light of deflection, impulsive velocity, von-Mises stresses, compression and tension damage of concrete.

2 Constitutive Modelling

The inelastic behavior of concrete has been incorporated through concrete damage plasticity model and the model includes compressive and tensile behavior. The elastic and plastic behavior of steel reinforcement bar has been incorporated using Johnson-cook model includes the effect of state of stress, temperature and strain rate and discussed in this section.

2.1 Concrete Damaged Plasticity Model for Concrete

In finite element modelling, inelastic behaviour of concrete was defined by using concrete damaged plasticity model (CDP) providing a general capability for modelling concrete and other quasi-brittle materials. The plastic-damage model is a form of plasticity theory in which a plastic-damage variable '*K*' was defined which increases if plastic deformation takes place. Moreover, the plastic-damage variable is limited to a maximum value and the attainment of this value at a point of the solid represents total damage, which can be interpreted as the formation of a macroscopic crack. The variable "*K"* is non-dimensional and its maximum value is unity. The concrete damaged plasticity model is a continuum, plasticity-based, damage model for concrete. The model assumes that the two main failure mechanisms are tensile cracking and compressive crushing of the concrete material. The evolution of the yield surface is controlled by two hardening variables which are linked to failure mechanisms under tension and compression loading, namely ε_c^{pl} and ε_t^{pl} are compressive and tensile equivalent plastic strains, respectively. The damage variables can take values from zero to one, where zero represents the undamaged material and one represents total loss of strength. The stress strain relations under uniaxial compression and tension loading are given by the following equations where E_o is the initial (undamaged) elastic stiffness of the material: $\sigma_t = (1-d_t)E_o(\varepsilon_t-\varepsilon_t^{pl})$ and $\sigma_c = (1-d_c)E_o(\varepsilon_c-\varepsilon_c^{pl})$, where d_t and d_c are tension damage variable and compression damage variable respectively [13]. The concrete damaged plasticity model parameters such as (d_t) tension and (d_c) compression damage variables are shown in Tables 1 and 2. The ratio between initial equi-biaxial compressive yield stress (fb_o) to initial uniaxial compressive yield stress (fc_o) i.e. fb_o/fc_o was considered as 1.16 [13-14]. The compressive strength of concrete was considered 20 MPa and Poisson's ratio of the concrete was assumed equal to 0.18. The parameters for CDP model other than damage variables are shown in Table 3.

Table 1 - Compressive damage variables for CDP model

Yield Stress(MPa)	Inelastic Strain	Damage Parameter(d_c)
20	0	0
15	0.0011	0.2
12	0.004	0.24

Table 2 - Tensile damage variables for CDP model

Yield Stress(MPa)	Cracking Strain	Damage Parameter(d_t)
3.3	0	0
3.2	0.003	0.15
3.1	0.005	0.21
3.0	0.007	0.28
2.95	0.01	0.30

Table 3 - Concrete damaged plasticity model values of concrete

Description	Numerical value
Elastic Modulus, E (GPa)	24
Dilation Angle	30
Flow Potential Eccentricity	1
Viscosity Parameter	0.1
Bulk Modulus, K	0.666
fb_o/fc_o	1.16

2.2 Johnson-Cook model for Reinforcement

The flow and fracture behavior of projectile and target material was predicted employing the Johnson-Cook elasto-viscoplastic material model [15] available in ABAQUS finite element code. The material model is based on the von Mises yield criterion and associated flow rule. It includes the effect of linear thermo-elasticity, yielding, plastic flow, isotropic strain hardening, strain rate hardening, softening due to adiabatic heating and damage. The Johnson and Cook [15] extended the

failure criterion proposed by Hancock and Mackenzie [16] by incorporating the effect of strain path, strain rate and temperature in the fracture strain expression, in addition to stress triaxiality. The fracture criterion is based on the damage evolution wherein the damage of the material is assumed to occur when the damage parameter, exceeds unity: The strain at failure is assumed to be dependent on a non-dimensional plastic strain rate, a dimensionless pressure-deviatoric stress ratio, (between the mean stress and the equivalent von-Mises stress) and the non-dimensional temperature, defined earlier in the Johnson-Cook hardening model. When material damage occurs, the stress-strain relationship no longer accurately represents the material behavior, ABAQUS [17]. The use of stress-strain relationship beyond ultimate stress introduces a strong mesh dependency based on strain localization i.e., the energy dissipated decreases with a decrease in element size. Hillerborg's fracture energy criterion has been employed in the present study to reduce mesh dependency by considering stress-displacement response after the initiation of damage. The section of the reinforcement is assigned Fe250 steel and the ultimate tensile strength is 250 MPa is approximately equivalent to the ultimate tensile strength proposed by Iqbal et al. [18]. The material properties of the steel reinforcing bar has been shown in Table 4.

Table 4 - Material parameters for steel reinforcing bar

Description	Notations	Numerical value
Modulus of elasticity	E (N/mm^2)	203000
Poisson's ratio	V	0.33
Density	ρ (Kg/m^3)	7850
Yield Stress constant	A (N/mm^2)	304.330
Strain hardening constant	B (N/mm^2)	422.007
	n	0.345
Viscous effect	C	0.0156
Thermal softening constant	m	0.87
Reference strain rate	$\dot{\varepsilon}_0$	.0001 s^{-1}
Melting temperature	θ_{melt} (K)	1800
Transition temperature	$\theta_{transition}$ (K)	293
Fraction strain constant	D_1	0.1152
	D_2	1.0116
	D_3	-1.7684
	D_4	-0.05279
	D_5	0.5262

3 Finite Element Modelling

The finite element model of the reinforced concrete frame was made using ABAQUS/CAE. The length, breadth and width of building was considered 3 m and whereas the size of beam and column was 0.3 m, arbitrary. The thickness of roof slab was 120 mm, whereas the reinforced concrete wall all four sides was 0.2 m. The steel reinforcement of main bar on both column and beam was 4 number of 12 mm diameter was considered. The 8 mm diameter stirrups having two leg have been placed at 200 mm center to centre distance was considered. The steel reinforcement of concrete wall of all four sides was considered 10 mm diameter having spacing of 180 mm on both longitudinal and transverse direction of single mat. The size reinforcement on slab was considered as 8 mm diameter placed at 225 mm centre to centre distance on both the direction. The geometry of the concrete and steel reinforcement was modeled as solid deformable body. The interaction between concrete and steel was modeled using the tie constraint option available in ABAQUS/CAE wherein the concrete was assumed as host region and the steel as embedded region. The constitutive and fracture behavior of materials have been predicted using JC model available in ABAQUS. The combined model of building has been shown in Fig. 1(a) and the rotational and translational motion of the base of the building was restricted to depict rigid supports at the ends. The origin of blast was assumed at three different location, see Fig. 1(b). The origin of blast considered against location 1 was 2 m from the exterior surface of slab (Top Side) whereas location 2 was 2 m from exterior surface of wall (Front Side). The blast origin of location 3 was kept inside centre of the building and 1 m from the bottom of roof slab (Inside). The typical finite element modelling of steel reinforcement and concrete of wall element has been shown in Fig. 1(c)-(d). The typical finite element modelling of column, beam, slab and wall has been shown in Fig. 2(a)-(c) and assembled model is shown in Fig. 3. The concrete elements

of all the components were meshed using structured elements of 8 noded hexahedral linear brick element and steel reinforcement was meshed with linear truss element, see Figs. 1-3.

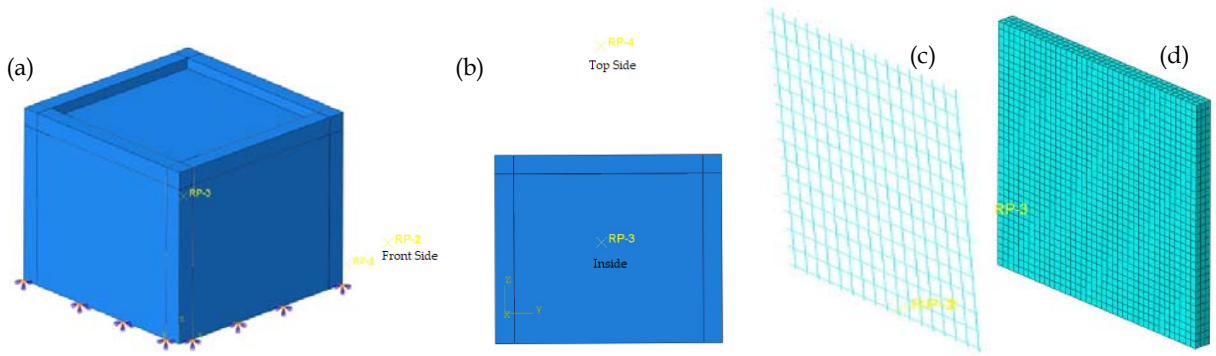

Fig. 1 - Building frame with (a) fixed boundary conditions, and (b) locations of blast, (c) Shear wall reinforcement, and (d) concrete

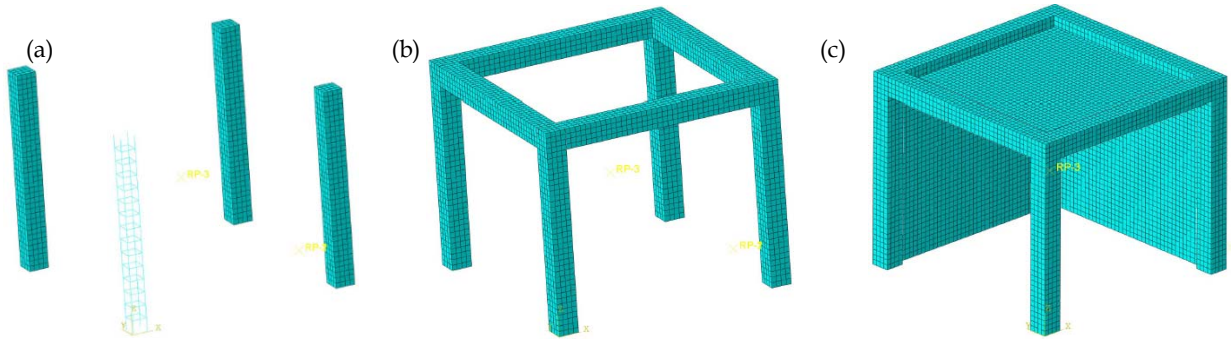

Fig. 2 - Building (a) columns with reinforcement (b) concrete frame and (c) frame with walls and roof slab

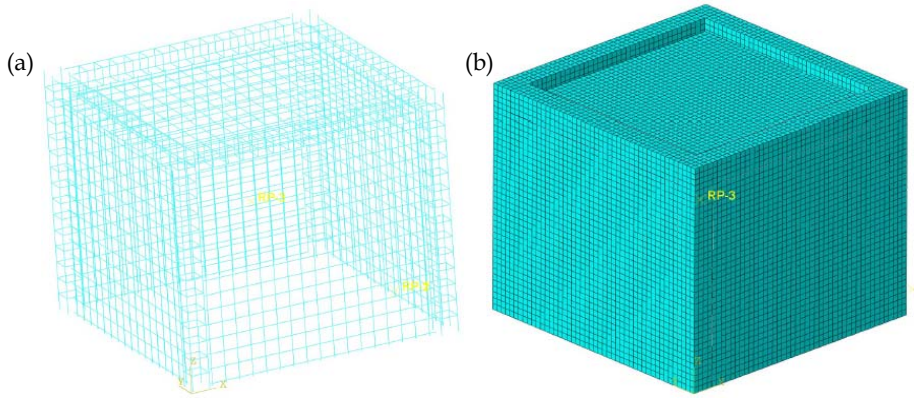

Fig. 3 - Profile of building (a) reinforcement and (b) concrete

The mesh convergence study has been carried out by varying the mesh sizes of 100, 80, 60, 40 and 30 mm, were considered equal size for beam, column, slab as well as reinforcement. The displacement and von-Mises stresses of structural members of varying mesh against blast load of 20 kg mass TNT originated (location 1) inside of building is shown in Figs. 4 and 5, respectively. The maximum deflection was found to be 160, 182, 181, 199 and 204 mm against 100, 80, 60, 40 and 30 mm respectively, see Fig. 4. The von-Mises stresses in concrete were found to be 13.6, 18.8, 21.2, 26.1 and 26.8 MPa against 100, 80, 60, 40 and 30 mm respectively, see Fig. 5. The von-Mises stresses in steel reinforcing bar were found to be 439, 391, 431, 407 and 401 MPa against 100, 80, 60, 40 and 30 mm respectively. The size of mesh for concrete slab, beam

and wall have been considered as 80 × 80 × 80 mm. On the basis of prediction of displacement, it is clearly seen that increment of deflection is insignificant when the mesh size is decreased below 80 mm. Also, the variation of Mises stresses on both steel reinforcing bar as well as concrete is insignificant when the mesh size is decreased below 80 mm. Overall, it is found that the results were not found to be mesh sensitive due to the small size of elements which were already chosen. However, the size of element chosen in the present study was slightly larger due to relatively larger number of elements as well as longer computational time. The corresponding reinforcing steel elements size 80 mm was assigned, giving a total number of 23,256 elements of slab concrete and 6,840 elements of steel reinforcement bar. The analysis was divided into 20 frames within a time frame of 0.08 second. A typical simulation for blast event took around 20 CPU minutes. The blast load was incorporated using interaction module available in ABAQUS. In general, the structure can be analysed against surface blast or air blast, however in the present study surface blast was considered. The surface blast load was created using CONWEP definition and the surface blast was consigned with help of two reference point which is assigned based on standoff distance from point of response.

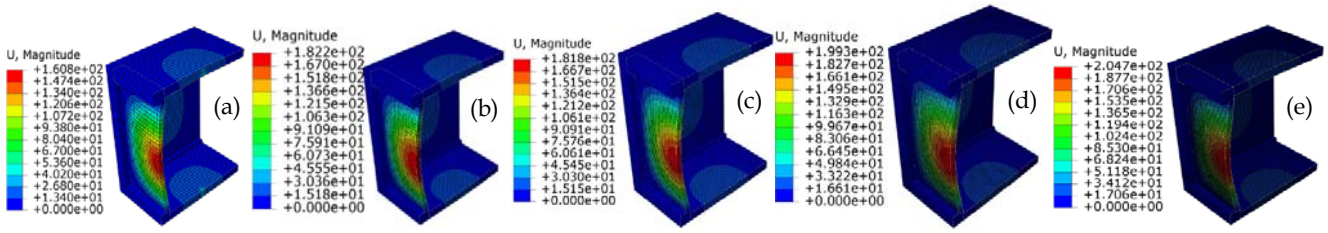

Fig. 4 - Deflection of the systems against (a) 100, (b) 80, (c) 60, (d) 40, and (e) 30 mm mesh size

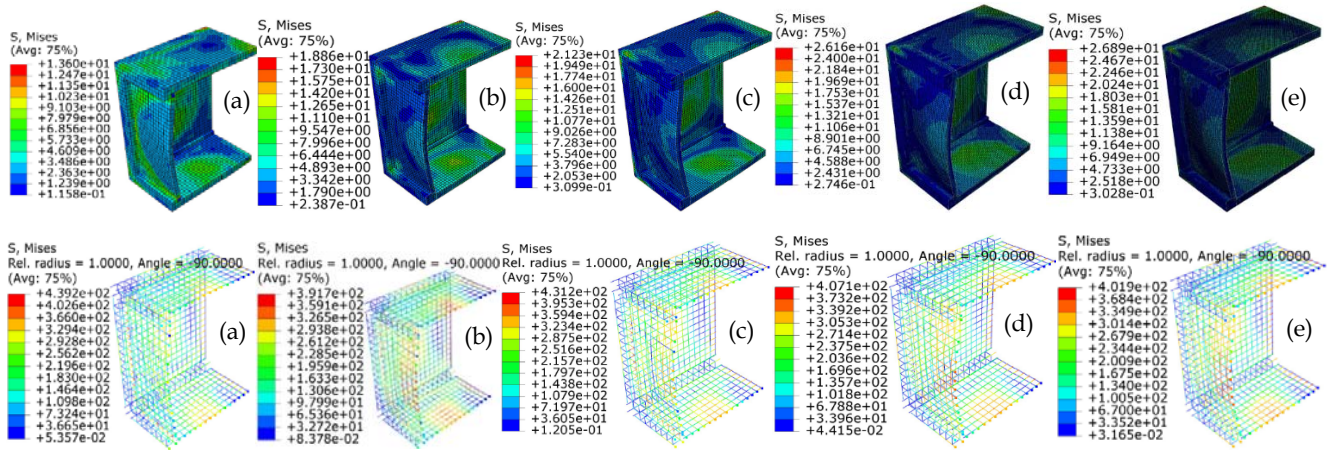

Fig. 5 - Von-Mises stresses in concrete and steel reinforcement against (a) 100, (b) 80, (c) 60, (d) 40, and (e) 30 mm mesh size

4 Results and Discussion

Three-dimensional finite element analysis has been carried out in order to study the effect of monolithic reinforced concrete building using ABAQUS/CAE. The responses of structure and structural elements against blast loading has been discussed here. The simulations were carried out against varying standoff distance, mass of TNT, locations of blast origin and thickness of roof slab. The response of structural elements were studied in light of deflection, impulsive velocity, von-Mises stresses, and compression and tension damage of concrete therein were presented and discussed.

4.1 Influence of varying mass of TNT

The simulations were carried out against varying mass of TNT and locations of blast origin. In the present study, the mass of TNT was considered as 2, 5, 10 and 20 kg against varying standoff distance. The origin of blast has been considered

against location 1 and was fixed at 2 m from the exterior surface of slab (Top Side) whereas location 2 was fixed 2 m from exterior surface of wall (Front Side) were discussed in this Section. The blast origin of location 3 was fixed (inside) at centre of the building and 1 m from the bottom of roof slab is discussed in this Section.

4.1.1 Inside of building

The von-Mises stress on concrete and steel reinforced bar of the members against blast load of varying mass TNT originated (location 1) inside of building is shown in Fig. 6(a)-(d). The unit of the von-Mises stress in the contours, "N/mm^2". The maximum von-Mises stress at the concrete was found to be 5.45, 10.95, 10.83 and 18.86 MPa for 2, 5, 10 and 20 kg mass respectively. The von-Mises stress at the steel reinforced bar was found to be 326, 374, 376 and 391 MPa for 2, 5, 10 and 20 kg mass respectively. It is observed that the stress developed in the wall was found to be higher than the roof slab and it may be due to the rigidity and stiffness of the wall. The maximum stress in steel bar and concrete was about 391 and 18.86 Mpa against mass of 20 kg TNT respectively and it is found to be more vulnerable.

The displacement of structural members against blast load of varying mass TNT originated (location 1) inside of building is shown in Fig. 7(a)-(d). The unit of the displacement contours was "millimeter". The maximum deflection was found to be 12, 41, 90 and 182 mm against 2, 5, 10 and 20 kg mass TNT respectively. It is observed that the deflection developed in the roof slab was found to be higher than the wall and the reason may be due to the thickness of slab less as compared to the wall thickness. The maximum deflection on roof slab was about 182 mm against mass of 20 kg TNT and it is found to be more vulnerable. The deflection of slab against 20 kg mass was found to be increased 93, 77 and 50% as compared to the deflection of slab by 2, 5 and 10 kg mass TNT respectively.

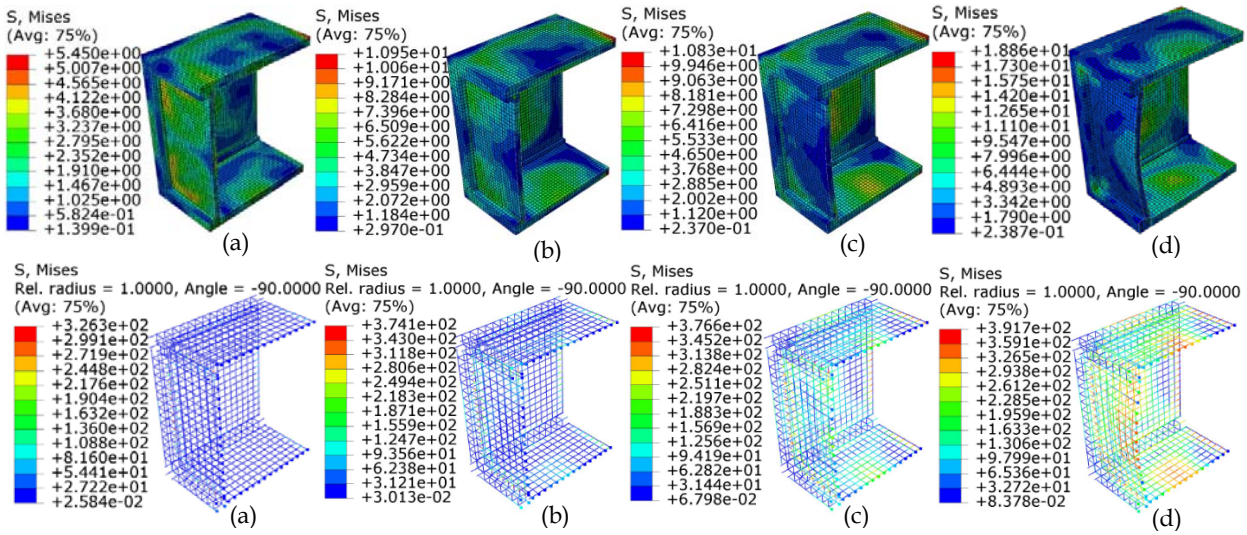

Fig. 6 - Von-Mises stresses in concrete and steel reinforcement against (a) 2, (b) 5, (c) 10, and (d) 20 kg mass TNT

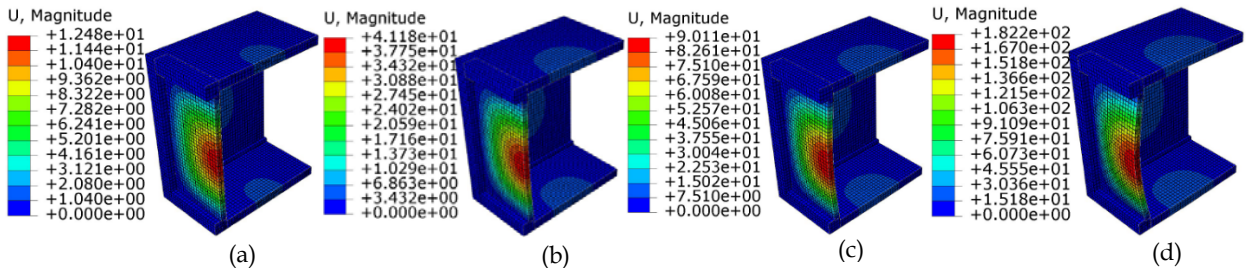

Fig. 7 - Deflection of building frame against (a) 2, (b) 5, (c) 10, and (d) 20 kg mass TNT

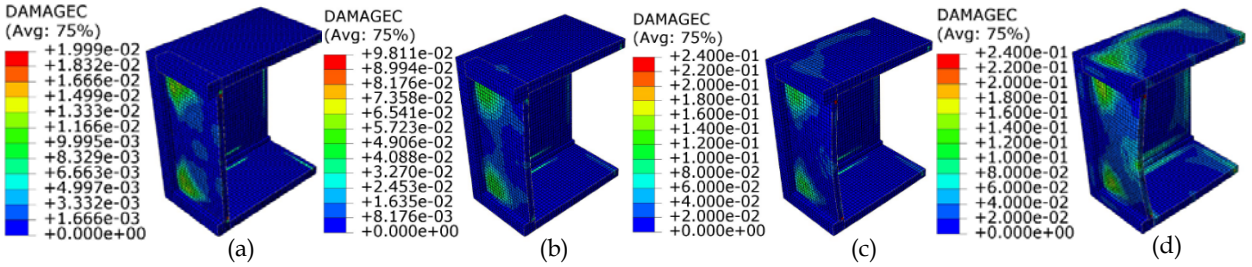

Fig. 8 - Compression damage of concrete against (a) 2, (b) 5, (c) 10, and (d) 20 kg mass TNT

The compression damage of structural members against blast load of varying mass TNT originated (location 1) inside of building is shown in Fig. 8(a)-(d). The unit of the displacement contours was "nil". The maximum damage due to compression was found to be 0.019, 0.098, 0.24 and 0.24 for 2, 5, 10 and 20 kg mass respectively. The compression damage parameter was considered maximum of 0.24 in the present study. Therefore, it is observed that the compression damage in the roof slab against 10 kg mass TNT was found maximum. Therefore, it is concluded that the building was found to be more vulnerable against 10 kg mass of TNT. The damage criteria against 10 kg mass was found to be increased 92 and 60% as compared to the damage criteria by 2 and 5 kg mass TNT respectively.

4.1.2 Front of building

The von-Mises stress on concrete and steel reinforced bar of the members against blast load of varying mass TNT originated (location 2) front side of building is shown in Fig. 9(a)-(d). The maximum von-Mises stress at the concrete was found to be 6.34, 11.7, 10.28 and 10.94 MPa for 2, 5, 10 and 20 kg mass respectively. The von-Mises stress at the steel reinforced bar was found to be 49, 212, 322 and 354 MPa for 2, 5, 10 and 20 kg mass respectively. It is observed that the stress developed in the concrete was found to be almost same. The stresses in steel reinforcement due to 5 kg mass TNT was found increased almost four times as compared to 2 kg mass TNT. However the stress in the steel reinforcement was found to be increased with increase on mass of TNT. The maximum stress in steel bar was about 354 Mpa against mass of 20 kg TNT and it is found to be more severe.

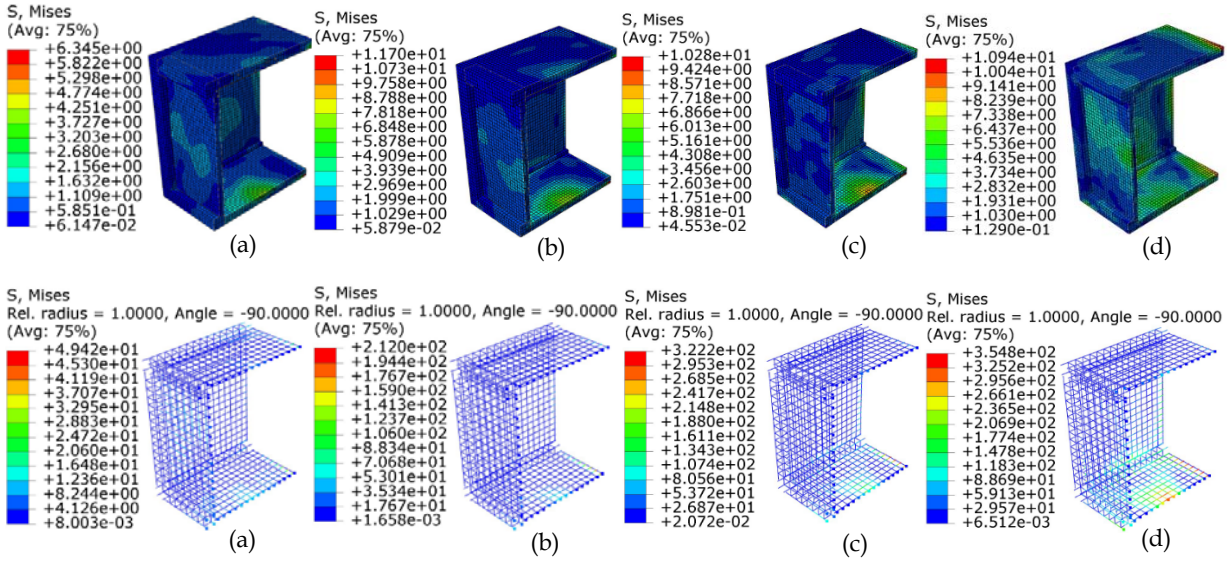

Fig. 9 - Von-Mises stresses "(N/mm^2) in concrete and steel bar against (a) 2, (b) 5, (c) 10, and (d) 20 kg TNT

The displacement of structural members against blast load of varying mass TNT originated (location 2) front side of building is shown in Fig. 10(a)-(d). The maximum deflection was found to be 0.5, 1.5, 5.7 and 16 mm against 2, 5, 10 and 20 kg mass respectively. Overall, the deflection developed in the roof slab as well as wall was found to be insignificant. The maximum deflection on roof slab was about 16 mm against mass of 20 kg TNT. It is observed that the target influenced by local indentation against 10 and 20 kg mass whereas the target experienced the global indentation against 2 and 5 kg mass TNT. At 2 kg mass TNT, both the wall experienced deformation whereas, the pattern of deformation decreased at 5 kg mass

TNT. At 10 and 20 kg mass TNT, the occurrence of deformation only at front side and it may be due to the impulse velocity dissipates entirely by front side wall.

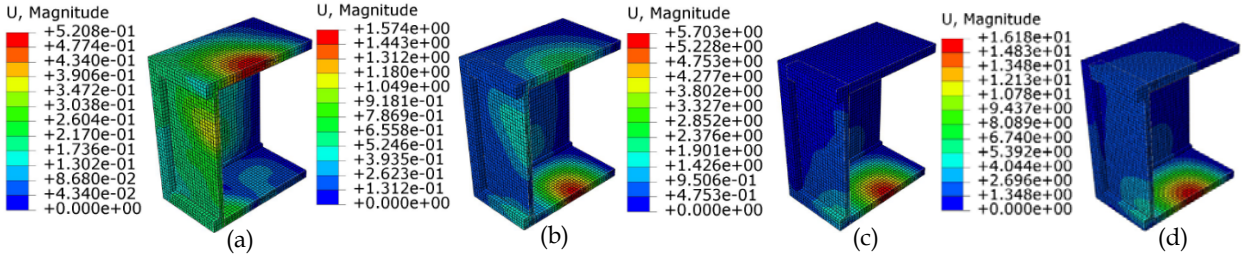

Fig. 10 - Deflection (mm) of building frame against (a) 2, (b) 5, (c) 10, and (d) 20 kg mass TNT

The compression damage of structural members against blast load of varying mass TNT originated (location 2) front side of building is shown in Fig. 11(a)-(d). The maximum damage due to compression was found to be 0.002, 0.014, 0.04 and 0.12 for 2, 5, 10 and 20 kg mass respectively. The compression damage parameter was considered 0.24 in the present study however target experienced maximum of 0.12 against 20 kg mass TNT. It is observed that the compression damage was found to be maximum only at front side wall, see Fig. 11(a)-(d). Therefore, it is concluded that the structure was found to be safe against given mass of TNT if the blast originated 2 m from the front of building.

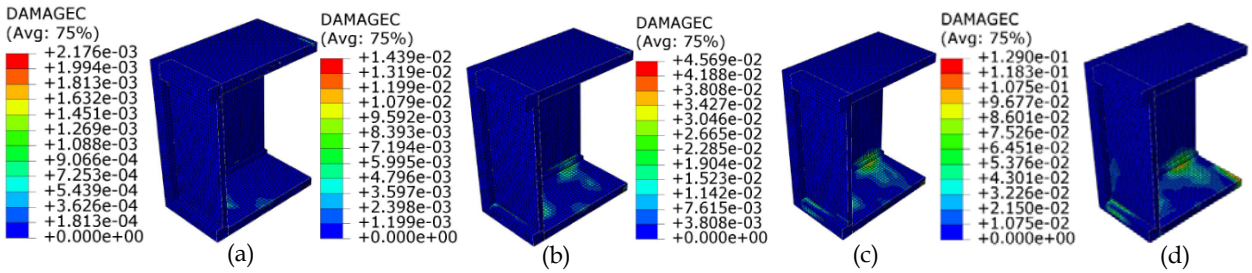

Fig. 11 - Compression damage of concrete against (a) 2, (b) 5, (c) 10, and (d) 20 kg mass TNT

4.1.3 Top of building

The von-Mises stress on concrete and steel reinforced bar of the members against blast load of varying mass TNT originated (location 3) top side of building is shown in Fig. 12(a)-(d). The maximum von-Mises stress at the concrete was found to be 4.29, 4.72, 7.18 and 10.24 MPa for 2, 5, 10 and 20 kg mass respectively. At 2 and 5 kg mass TNT, the stress developed in the concrete was found to be almost same. At 10 and 20 kg mass TNT, the stress found to be increased to 67 and 138% respectively as compared to 2 kg mass TNT. The von-Mises stress at the steel reinforced bar was found to be 118, 253, 276 and 333 MPa against 2, 5, 10 and 20 kg mass TNT respectively. The stress in steel reinforcement was found increased almost two times when the mass of TNT increased from 2 to 5 kg. However, at 5 and 10 kg mass TNT, the stress developed in the steel reinforcing bar was found to be almost same. Overall, the stress in the steel reinforcement was found to be increased with increase of mass of TNT. The maximum stress in steel bar was about 333 Mpa against mass of 20 kg TNT and it is found to be more severe.

The displacement of structural members against blast load of varying mass TNT originated (location 2) front side of building is shown in Fig. 13(a)-(d). The maximum deflection was found to be 4.3, 11, 26 and 67 mm against 2, 5, 10 and 20 kg mass respectively. The deflection developed in the roof slab was found to be significant, since the origin of blast close to the slab. The maximum deflection on roof slab was about 67 mm against mass of 20 kg TNT. It is observed that the target influenced by local indentation against given mass of TNT.

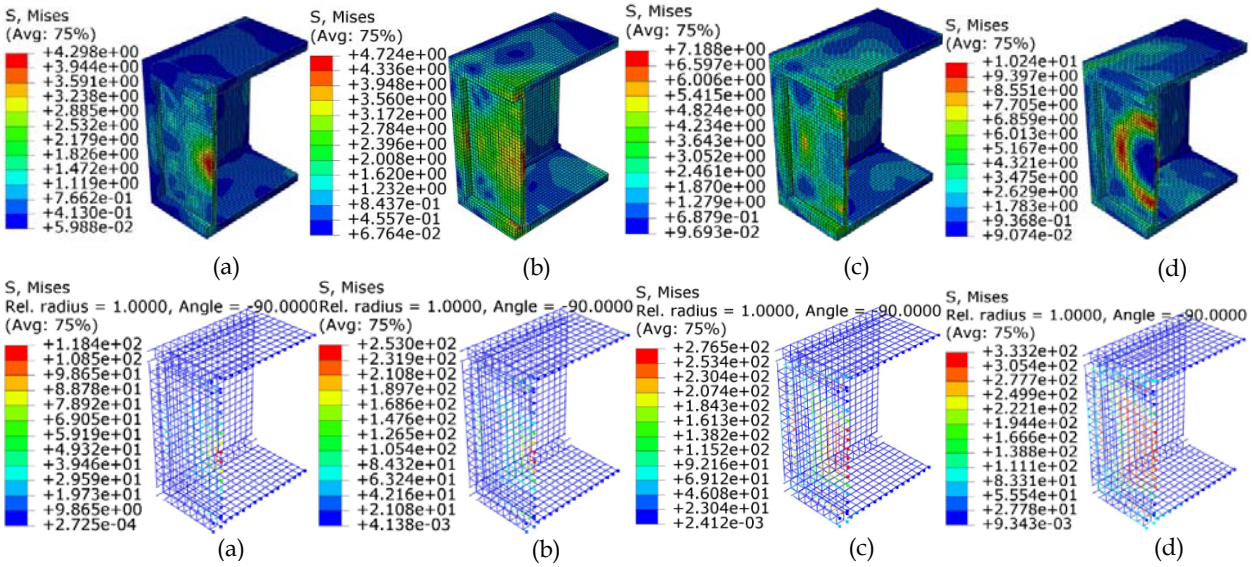

Fig. 12 - Von-Mises stresses in concrete and steel reinforcement against (a) 2, (b) 5, (c) 10, and (d) 20 kg mass TNT

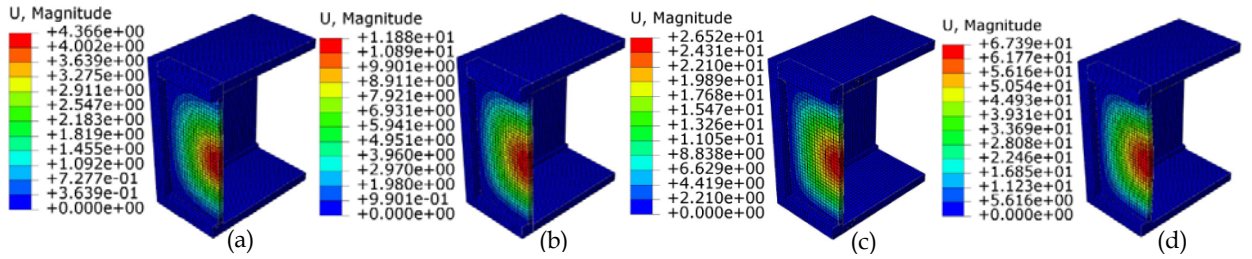

Fig. 13 - Deflection of building frame against (a) 2, (b) 5, (c) 10, and (d) 20 kg mass TNT

The compression and tension damage of structural members against blast load of varying mass TNT originated (location 3) top side of building is shown in Fig. 14(a)-(d). The maximum damage due to compressive impulsive load was found to be 0.003, 0.020, 0.053 and 0.145 for 2, 5, 10 and 20 kg mass respectively, see Fig. 14(a). The maximum damage due to tensile impulsive was found to be almost same, 0.3 against given mass of TNT, see Fig. 14(b). The compression damage parameter was considered maximum of 0.3 in the present study. The compression damage was considered 0.24 in the present study however target experienced maximum of 0.145 against 20 kg mass TNT.

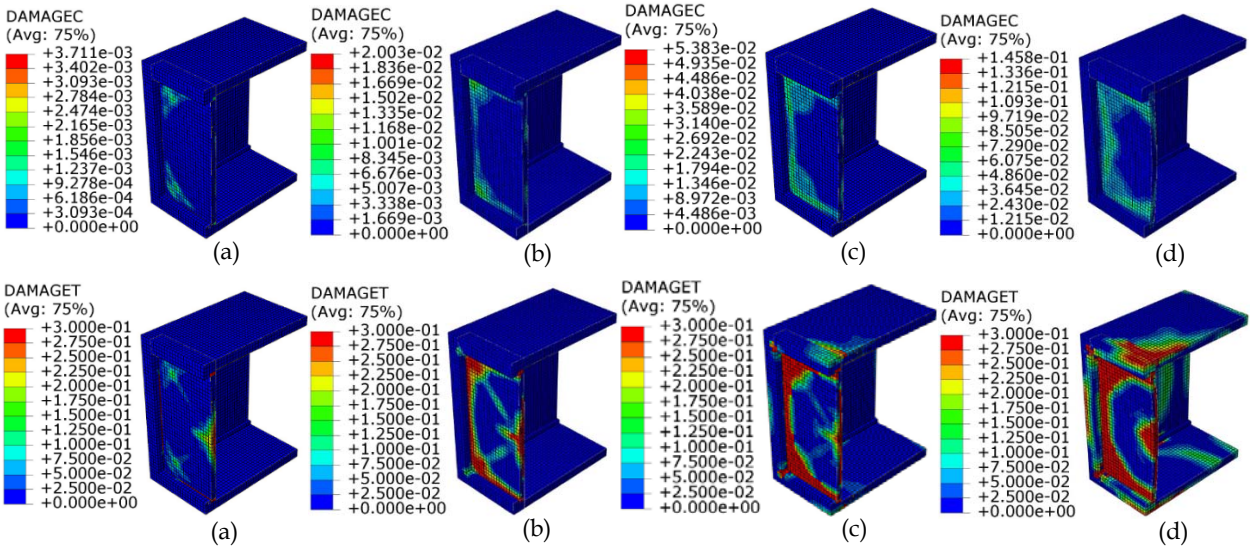

Fig. 14 - Compression and tension damage of concrete against (a) 2, (b) 5, (c) 10, and (d) 20 kg mass TNT

It is observed that the area of compression as well as tension damage was found increased significantly with increase of mass of TNT. It is observed that the compression as well as tension damage was found to be influenced only by roof slab due to varying mass of TNT. However, the roof slab as well as wall has been experienced significant damage against 20 kg mass TNT, see Fig. 14(d).

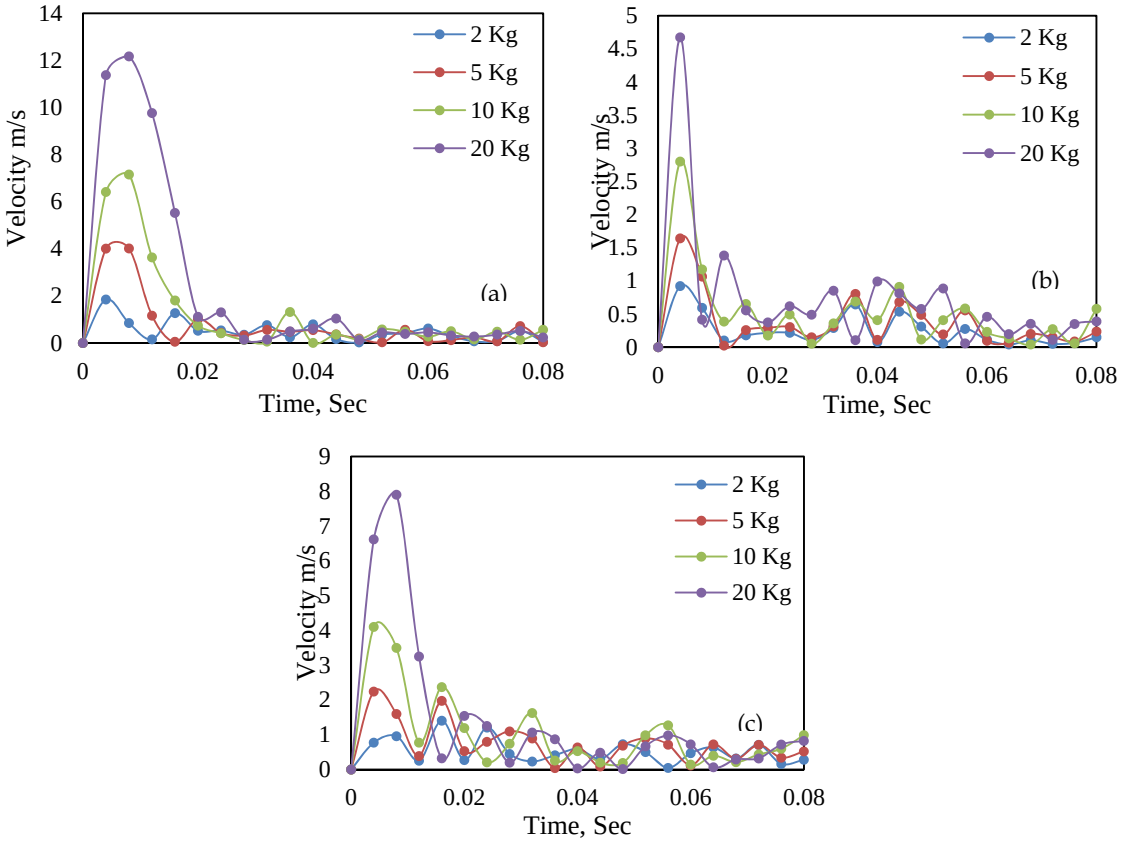

Fig. 15 - Velocity of impulse against different location of origin of blast at (a) inside (b) front and (c) top of the building

The impulse velocity due to the blast originated at different location (location 1, location 2 and location 3) and varying mass of TNT has been shown in Fig. 15(a)-(c). At location 1, the maximum impulse velocity 1.85, 4, 7.15 and 12.1 m/s against 2, 5, 10 and 20 kg mass respectively, see Fig. 15(a). At location 2, the maximum impulse velocity 0.9, 1.6, 2.8 and 4.6 m/s against 2, 5, 10 and 20 kg mass respectively, see Fig. 15(b). At location 3, the maximum impulse velocity 0.9, 2.2, 4.1 and 7.9 m/s against 2, 5, 10 and 20 kg mass respectively, see Fig. 15(c). Overall, it is observed that the impulsive velocity was found to increase with increase in mass of TNT. It is also observed that the impulsive velocity against blast location 1 was found to be maximum as compared to the location 2 and 3, see Fig. 15(a). The impulsive velocity against blast at location 1 was found to be higher, the reason may be due to the fact that the origin of blast was in closed chamber. Fig. 15(b) shows the velocity of impulse by the blast originated by location 2 was found to be significantly less as compared to location 1 and 3. The reason may be due to the fact that the origin of blast was in open space and blast wave travelling towards 200 mm thick wall. Fig. 15(c) shows the velocity of impulse by the blast originated by location 3 was found to be significantly higher as compared to location 2. The reason may be due to the fact that the origin of blast was in open space and blast wave travelling towards 120 mm thick wall. The duration of blast at location 1 was found to be 0.012, 0.016, 0.02 and 0.028 Second for 2, 5, 10 and 20 kg mass TNT respectively. However, the duration of blast at location 2 and 3 was found to be occurred small time period, i.e. 0.012 and 0.016 Seconds respectively.

4.2 Influence of standoff distance

The simulations were carried out against varying standoff distance to examine the resistance of structural elements. The standoff distance has been varied as 0.5 m, 1 m, 1.5 m and 2m. The response of structure in terms of von-Mises stress, deflection and compression damage have been discussed in this section. The von-Mises stress on concrete and steel reinforced

bar of the members against blast load of 20 kg mass TNT originated (location 2) front side of building is shown in Fig. 16(a)-(d). The maximum von-Mises stress at the concrete was found to be 12.7, 13. 8 13.3 and 10.94 MPa for 0.5, 1.0, 1.5 and 2.0 m standoff distance respectively. However the stress in the concrete was found to be increased with increase of standoff distance upto 1 m, thereafter the stress found to be decreased significantly. It is concluded that the stress developed in the concrete was found to be maximum when the standoff distance is 1 m. The von-Mises stress at the steel reinforced bar was found to be 410, 371, 370 and 354 MPa for 2, 5, 10 and 20 kg mass respectively. The stresses in steel reinforcement due to 0.5 m standoff distance was found increased almost 20% as compare to 2 m. Overall, it was found that as the standoff distances decrease the von-Mises stresses in steel increased. Therefore, nearer the location of blast from the structure, more severe in its effect.

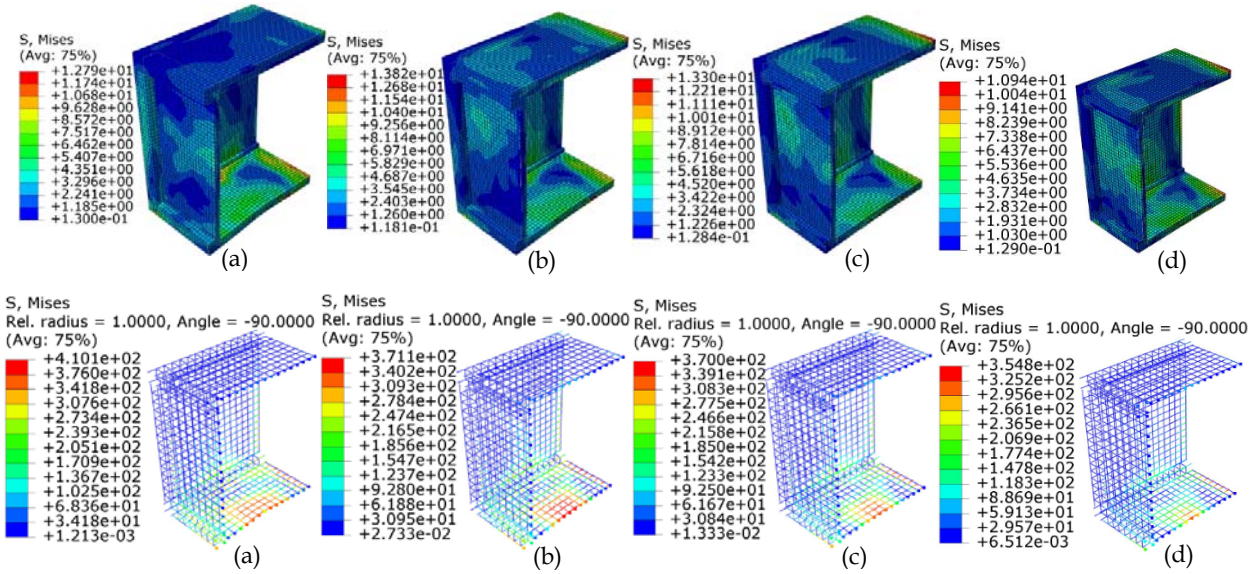

Fig. 16 - Von-Mises stresses in concrete and steel reinforcement against (a) 0.5, (b) 1.0, (c) 1.5, and (d) 2.0 m standoff distance

The displacement of structural members against blast load of varying mass TNT originated (location 2) front side of building is shown in Fig. 17(a)-(d). The maximum deflection was found to be 96, 41, 25 and 16 mm against 0.5, 1.0, 1.5 and 2.0 m standoff distance respectively. Overall, the deflection developed in the roof slab as well as other side of reinforced concrete wall was found to be insignificant. The maximum deflection on wall was about 96 mm against 0.5 m standoff distance. It is observed that the target influenced by local indentation against 0.5 m standoff distance whereas the target experiencing the global indentation that is to be increased with increase of standoff distance, see Fig. 16. At 1.5 and 2.0 m standoff distance, the slab as well as wall of other side has also experienced deformation, see Fig. 17(c)-(d). The results of deflection indicate that the standoff distance has great influence on the survivability of reinforced concrete slab and wall.

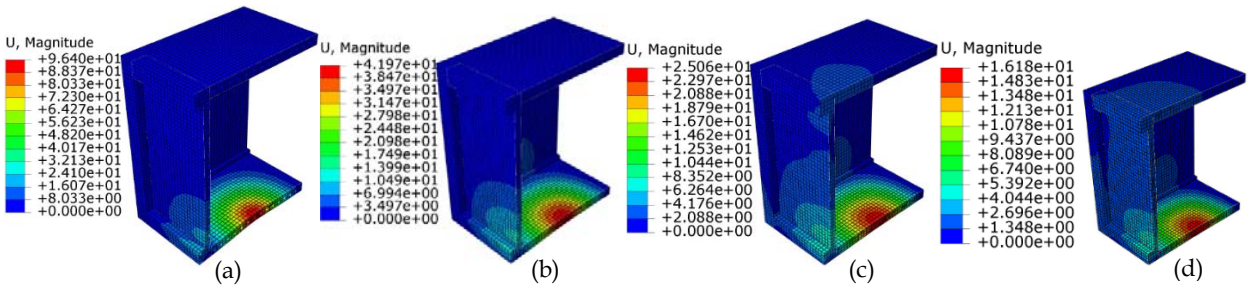

Fig. 17 - Deflection of building frame against (a) 0.5, (b) 1.0, (c) 1.5, and (d) 2.0 m standoff distance

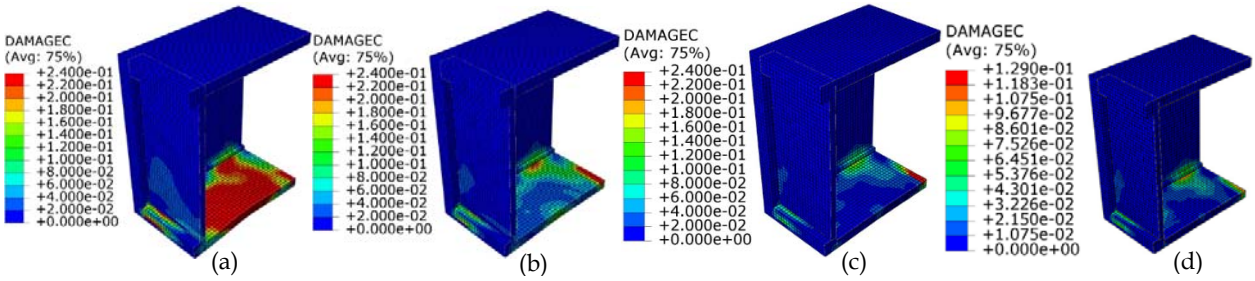

Fig. 18 - Compression damage of concrete against (a) 0.5, (b) 1.0, (c) 1.5, and (d) 2.0 m standoff distance

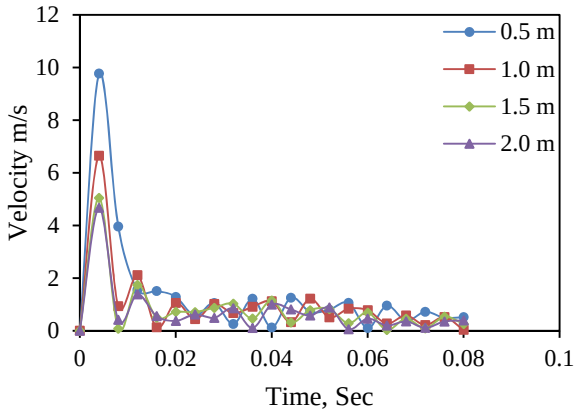

Fig. 19 - Velocity of impulse against varying standoff distance

The compression damage of structural elements against blast load of 20 kg mass TNT originated (location 2) at front side of building is shown in Fig. 18(a)-(d). The maximum damage due to compression was found to be 0.24, 0.24, 0.24 and 0.129 for 0.5, 1.0, 1.5 and 2.0 m standoff distance respectively. The compression damage parameter was considered 0.24 in the present study however target experienced maximum of 0.24 against 0.5, 1 and 1.5 m standoff distance. At 0.5 m standoff distance, it is observed that the compression damage was found to be maximum only at front side wall, see Fig. 18(a). Therefore, it is concluded that the structure was found to be safe against 20 kg mass of TNT and the blast takes place 2 m away from the front of building. The impulse velocity due to the blast originated at location 2 and 20 kg mass of TNT has been shown in Fig. 19. The maximum impulse velocity 9.7, 6.6, 5.0 and 4.6 m/s against 0.5, 1.0, 1.5 and 2.0 m standoff distance respectively. Overall, it is observed that the impulsive velocity was found to increase with decrease of standoff distance. The duration of blast was found to be 0.008 second.

4.3 Influence of thickness of wall

The simulations were carried out against varying thickness of roof slab to examine the resistance of structural elements. The thickness of roof slab has been varied as 200 and 120 mm. The response of structure in terms of von-Mises stress, deflection and compression damage have been discussed in this section. The von-Mises stress on concrete and steel reinforced bar of the members against blast load of 50 kg mass TNT originated (location 2) at front side of building is shown in Fig. 20(a)-(b). The maximum von-Mises stress at the concrete was found to be almost same, i.e. 28 MPa for both the slab. It is observed that the stress developed in the concrete of both the thickness was found to be maximum when the mass of TNT 50 kg. The von-Mises stress at the steel reinforced bar was found to be 464 and 439 MPa for 120 and 200 mm thickness respectively. The stresses in steel reinforcement of 200 mm thick slab was found decreased only 6% as compare to 120 mm thick slab. Therefore, it is concluded that the thickness of slab does not influece when the mass of TNT is high and the structure influence more severe in its effect.

The displacement of structural members against blast load of 50 kg mass TNT originated (location 2) at front side of building is shown in Fig. 21(a)-(b). The maximum deflection was found to be 438 and 110 mm by 120 and 200 mm thick slab respectively. In case of 120 mm thick slab, the deflection developed on only slab, it may be due to the fact that the stiffness and rigidity of 120 mm thick slab was less than the 200 mm thick slab. The distribution of intensity of displacement

of 120 mm slab was found to be significant as compared to other walls on four sides. It is observed that the target influenced by local indentation and damage on 120 mm thick slab whereas the target of 200 mm slab experiencing the global indentation of all four sides, see Fig. 21. The results of deflection indicate that the thickness of slab has great influence on the survivability of reinforced concrete slab and wall.

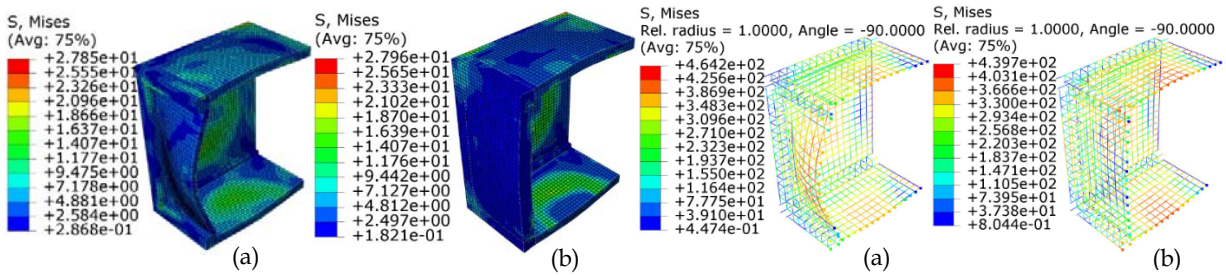

Fig. 20 - Von-Mises stresses in concrete and steel reinforcement of (a) 120 and (b) 200 mm thick slab

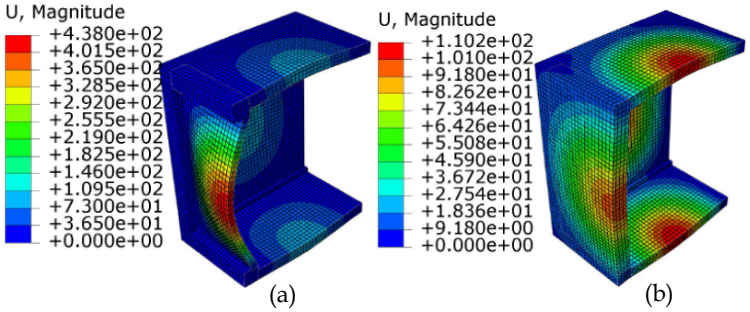

Fig. 21 - Deflection of building frame having (a) 120 and (b) 200 mm thick wall

5 Conclusion

The present study addresses the finite element investigation on the behavior of building and building elements to blast load of varying mass of TNT. The numerical simulations were carried out using ABAQUS/Explicit finite element model to predict the response of structures against surface blast induced impulse velocity. The response of the structure in terms of locations such as inside, front side and top side of building was studied against blast load which is introduced for different masses of TNT i.e. 2, 5, 10 and 20 kg. Also the response of structural elements was studied by varying standoff distance as 0.5, 1, 1.5 and 2.0 m against 20kg mass of TNT. Also the response of structure was studied by varying the thickness of slab and the following conclusions have been drawn.

The stress in steel reinforcement and concrete was 391 and 18.86 Mpa against blast by mass of 20 kg TNT respectively and it is found to be more vulnerable as compared to location 2 and 3. The maximum deflection on roof slab was 182, 16 and 67 mm by the blast location 1, 2 and 3 respectively. It is also observed that the impulsive velocity against blast location 1 was found to be maximum as compared to the location 2 and 3. The impulsive velocity against blast at location 1 was found to be higher, the reason may be due to the fact that the origin of blast was in closed chamber. The stresses in steel reinforcement due to 0.5 m standoff distance was found to be increased 20% as compared to 2 m, however the stress on concrete was found to be almost same. It is observed that the target influenced by local indentation and 96 mm displacement against blast of 0.5 m standoff distance whereas the target experiencing the global indentation that is to be increased with increase of standoff distance. The maximum damage due to compression was found to be almost same upto 1.5 m standoff distance. The results of deflection indicate that the standoff distance has great influence on the survivability of reinforced concrete slab and wall. The maximum von-Mises stress at the concrete was found to be almost same, i.e. 28 MPa for both 200 as well as 120 mm thick slab. The stresses in steel reinforcement of 200 mm thick slab was found decreased only 6% as compare to 120 mm thick slab. Therefore, it is concluded that the thickness of slab does not influence when the mass of TNT is high and the structure influence more severe in its effect.

REFERENCES

[1]- H.M. Elsanadedy, T.H. Almusallam, H. Abbas, Y.A. Al-Salloum, S.H. Alsayed, Effect of blast loading on CFRP-Retrofitted RC columns – A numerical study. Lat. Am. J. Solids Struct. 8(2011) 55 – 81. doi:10.1590/S1679-78252011000100004

[2]- J.E. Crawford, L.J. Malvar, J.W. Wesevich, J. Valancius, A.D. Raynolds, Retrofit of reinforced concrete structures to resist blast effects. ACI Struct. J. 94(4) (1997) 371–377.

[3]- S. Ahmad, M. Taseer, H. Pervaiz, Effects of impulsive loading on reinforced concrete structure. Tech. J. UET Taxila, Vibration analysis, special issue, (2012) 9-23.

[4]- S.C. Woodson, W.H. Gaube, T.C. Knight, Alternative shear reinforcement guidelines for blast-resistant design, U.S. Army Engineer Waterways Experiment Station, 3909 Halls Ferry Road, Vicksburg, MS, 39180 (1990) 1-22.

[5]- Y. Shi, Z-X. Li, H. Hao. Bond slip modelling and its effect on numerical analysis of blast-induced responses of RC columns. Struct. Eng. Mech. 32(2) (2009) 251–267. doi:10.12989/sem.2009.32.2.251

[6]- E.A. Samir, Finite element analysis of reinforced concrete columns under different range of blast loads. Int. J. Civ. Struct. Eng. 5(2) (2014) 155-164. doi:10.6088/ijcser.2014050015

[7]- K.W. King, J.H. Wawclawczyk, C. Ozbey, Retrofit strategies to protect structures from blast loading. Can. J. Civil Eng. 36(8) (2009) 1345–1355. doi:10.1139/L08-058

[8]- T. Ngo, P. Mendis, A. Gupta, J. Ramsay, Blast Loading and Blast Effects on Structures – An Overview. Electron. J. Struct. Eng. Special Issue: Loading on Structures, (2007) 76-91.

[9]- S. Watson, W.N. MacPherson, J.S. Barton, J.D.C. Jones, A. Tyas, A.V. Pichugin, A. Hindle, W. Parkes, C. Dunare, T, Stevenson, Investigation of shock waves in explosive blasts using fibre optic pressure sensors. Meas. Sci. Technol. 17(6) (2005) 226–231.

[10]- M.R. Wakchaure, S.T. Borole, Comparison of maximum stress distribution of long & short side column due to blast loading. Int. J. Modern Eng. Res. 3(4) (2013) 1988-1993.

[11]- B.R. Ellis, D. Crowhurst, The response of several LPS maisonettes to small gas explosions. ISE/BRE Seminar: Structural design for Hazardous Loads: The Role of Physical Tests, Brighton, 1991.

[12]- J. Sagaseta, P. Olmati, K. Micallef, D. Cormie, Punching shear failure in blast-loaded RC slabs and panels. Eng. Struct. 147(2017) 177-194. doi:10.1016/j.engstruct.2017.04.051

[13]- K. Senthil, S. Rupali, K.S. Satyanarayanan, Experiments on ductile and non-ductile reinforced concrete frames under static and cyclic loading. J. Coupled Syst. Multiscale Dyn. 5(1) (2017) 38-50. doi:10.1166/jcsmd.2017.1118

[14]- M.A. Iqbal, S. Rai, M.R. Sadique, P. Bhargava, Numerical simulation of aircraft crash on nuclear containment structure. Nucl. Eng. Des. 243(2012) 321-335. doi:10.1016/j.nucengdes.2011.11.019

[15]- G.R. Johnson, W.H. Cook, Fracture characteristics of three metals subjected to various strains, strain rates, temperatures, and pressures. Eng. Fract. Mech. 21(1) (1985) 31–48. doi:10.1016/0013-7944(85)90052-9

[16]- J.W. Hancock, A.C. Mackenzie, On the mechanisms of ductile failure in high-strength steels subjected to multi-axial stress-states. J. Mech. Phys. Solids. 24(2-3) (1976) 147–169. doi:10.1016/0022-5096(76)90024-7

[17]- ABAQUS, V., 2010. 6.14 Documentation. Dassault Systemes Simulia Corporation.

[18]- M.A. Iqbal, K. Senthil, P. Bhargava, N.K. Gupta, The characterization and ballistic evaluation of mild steel. Int. J. Impact Eng. 78(2015) 98-113. doi:10.1016/j.ijimpeng.2014.12.006